VALIDATION AND APPLICATION OF CFD MODELING FOR PREDICTING TRAFFIC INDUCED AIR POLLUTION IN A COMPLEX URBAN AREA

J5.4

Hong HUANG*, Ryozo OOKA, Shinsuke KATO, Taifeng JIANG,
Takeo TAKAHASHI, Takeaki WATANABE
Institute of Industrial Science, The University of Tokyo, Japan

1. INTRODUCTION

During the last several decades, a great many urban areas throughout the world have experienced significant growth in terms of urbanization and industrial activities. Such urban development, accompanied with increase in population and housing density, reduction of land resource and growth of transportation load, has given negative effect on human health and resulted in various environmental problems. Among these, urban air pollution is causing serious concern. Meanwhile, the public's rapidly growing awareness of life quality and sustainable resource planning and management makes the control of air pollution an urgent task in urban environmental engineering nowadays.

Urban air pollution involves physical and chemical processes and depends on the total emissions, transport and transformation phenomena in the atmosphere. In this discipline, urban wind environment is essential to determine the pollutants dispersion characteristics under meteorological conditions. Traditional approaches to investigating wind effects on buildings and structures in both the past and present days have employed flow visualization and measurement using scaled models in meteorological or environmental wind tunnels. Full-scale field survey are sometimes carried out to provide data for wind loading on buildings and structures for to determine the characteristics of atmospheric wind which is needed to simulate the natural wind in wind tunnels (Kim 1999). Accompanying the revolutionary progress in numerical modeling and radical improvements in computational capacity, the application of CFD technique began to play an important role in urban climate engineering. It allows assessing the wind environment around a specified area even if the objective is only described on a blueprint. It also enables pollution dispersion characteristics to be scrutinized without real observation. However, there are several difficulties involving the practical use of CFD in urban terrain due to the sophistication of the geometrical topography, violent fluctuations of meteorological conditions and traffic load. Nevertheless, CFD methods are expected to give satisfactory results in terms of environmental issues, such as pedestrian level winds and dispersion of pollutants. On the other hand, it is thought that atmospheric stability conditions play a significant role in the dispersion of traffic generated pollutants (Nakamura et al, 1988; Kim et al, 2001; Vardoulakis et al, 2003; Huang et al, 2005).

In this paper, CFD simulation is validated by a field survey in a complex urban area, and the effect of atmospheric stability on the dispersion of the pollutants has been analyzed.

2. CFD MODEL DESCRIPTION

Air flow in urban environment issue is generally assumed to be three-dimensional and incompressible. As is already well known, the base of CFD is the Navier-Stokes (NS) equation set, expressed for turbulent flows in terms of suitably-averaged velocities and pressures to make them amenable to numerical solution without excessive computing overheads. The conventional and still most widely-used approach is time averaging, also described as Reynolds averaging, in which the NS equations are transformed as the Reynolds-Averaged Navier-Stokes (RANS) set (Gosman 1999). Moreover, the approach of the standard k-ε model(Launder and Spalding 1974), which is widely and practically useful, is adopted for solutions. Although the standard k-ε model shows some problem in the prediction of the wake phenomenon around buildings, such as the overestimate of turbulent kinetic energy around windward corner (Murakami et al, 1988), it stills has a good reputation for reliability in the field of wind engineering (Murakami, 1990) and air pollutant diffusion analysis (Huang et al. 2000). The effect of

* *Corresponding author address:* Hong Huang,
Institute of Industrial Science, The University of Tokyo,
4-6-1 Komaba, Meguro-ku, Tokyo, 153-8505, Japan
email: hhong@iis.u-tokyo.ac.jp

Table 1 Governing equations

Continuity equation

$$\frac{\partial \langle u_i \rangle}{\partial x_i} = 0 \tag{1}$$

Momentum equation

$$\frac{\partial \langle u_i \rangle}{\partial t} + \frac{\partial \langle u_i \rangle \langle u_j \rangle}{\partial x_j} = -\frac{1}{\rho}\frac{\partial \langle p \rangle}{\partial x_i} + \frac{\partial}{\partial x_j}\left(\nu \left(\frac{\partial \langle u_i \rangle}{\partial x_j} + \frac{\partial \langle u_j \rangle}{\partial x_i} \right) - \langle u_i' u_j' \rangle \right) - g_i \beta \left(\langle \theta \rangle - \theta_0 \right) \tag{2}$$

Temperature transport equation

$$\frac{\partial \langle \theta \rangle}{\partial t} + \frac{\partial \langle u_i \rangle \langle \theta \rangle}{\partial x_i} = \frac{\partial}{\partial x_i}\left(\alpha \frac{\partial \langle \theta \rangle}{\partial x_i} - \langle u_i' \theta' \rangle \right) \tag{3}$$

Species transport equation

$$\frac{\partial \langle C_i \rangle}{\partial t} + \frac{\partial \langle u_i \rangle \langle C_i \rangle}{\partial x_i} = \frac{\partial}{\partial x_i}\left(D \frac{\partial \langle C_i \rangle}{\partial x_i} - \langle u_i' C_i' \rangle \right) \tag{4}$$

Turbulent energy transport equation

$$\frac{\partial k}{\partial t} + \frac{\partial \langle u_j \rangle k}{\partial x_j} = P_k + G_k + D_k - \varepsilon \tag{5}$$

Turbulent dissipation rate equation

$$\frac{\partial \varepsilon}{\partial t} + \frac{\partial \langle u_j \rangle \varepsilon}{\partial x_j} = D_\varepsilon + \frac{\varepsilon}{k}\left(C_{\varepsilon 1} P_k + C_{\varepsilon 3} G_k - C_{\varepsilon 2} \varepsilon \right) \tag{6}$$

$$-\langle u_i' u_j' \rangle = \nu_t \left(\frac{\partial \langle u_i \rangle}{\partial x_j} + \frac{\partial \langle u_j \rangle}{\partial x_i} \right) - \frac{2}{3} k \delta_{ij} \tag{7}$$

$$\nu_t = C_\mu \frac{k^2}{\varepsilon} \tag{8}$$

$$-\langle u_i' \theta' \rangle = \frac{\nu_t}{\sigma_\theta}\frac{\partial \langle \theta \rangle}{\partial x_i} \tag{9}$$

$$-\langle u_i' C_i' \rangle = \frac{\nu_t}{\sigma_w}\frac{\partial \langle C_i \rangle}{\partial x_i} \tag{10}$$

$$P_k = -\langle u_i' u_j' \rangle \frac{\partial \langle u_i \rangle}{\partial x_j} \tag{11}$$

$$G_k = -g_i \beta \langle u_i' \theta' \rangle \tag{12}$$

$$D_k = \frac{\partial}{\partial x_j}\left(\frac{\nu_t}{\sigma_k}\frac{\partial k}{\partial x_j} \right) \tag{13}$$

$$D_\varepsilon = \frac{\partial}{\partial x_j}\left(\frac{\nu_t}{\sigma_\varepsilon}\frac{\partial \varepsilon}{\partial x_j} \right) \tag{14}$$

$\sigma_k = 1.0, \quad \sigma_\varepsilon = 1.3, \quad \sigma_\theta = 0.9, \quad \sigma_w = 0.9,$

$C_{\varepsilon 1} = 1.44, \quad C_{\varepsilon 2} = 1.92, \quad C_{\varepsilon 3} : 1.44(G_k > 0); 0(G_k < 0)$

buoyancy is considered using the Boussinesq approximation, and the extra terms (Gk in Table 1) in the k and □ equations are introduced to allow for the production of turbulence due to buoyancy and the effect of thermal stratification on the turbulence dissipation rate. The equations governing the mass and momentum transportation of wind flow are shown in Table 1 as Equations (1) ~ (14).

3. OUTLINE OF COMPUTATION

3.1 Topography Configuration of Objective Domain

Kawasaki city is between Yokohama and Tokyo city, in the Kanto region of Japan. It is well known as being a center for heavy industry and has been developed as an extent urbanized region, as illustrated in Fig. 1. The buildings here are of various geometrical configurations and functions, such as residential houses, commercial offices, shopping centers, heavy industrial facilities. All of these building blocks are seemingly integrated to form a big congregation. Intensive human and industrial activities in this area generate heavy transportation load and raise the concern of air pollution induced by traffic road. In addition, house colony with excessive density narrow the width of street canyons and give negative effect on pollutants dispersion more or less.

The analysis objective in this study is a small part of Kawasaki city, which is shown as the square region enclosed by black broken line in Fig. 1. It covers a

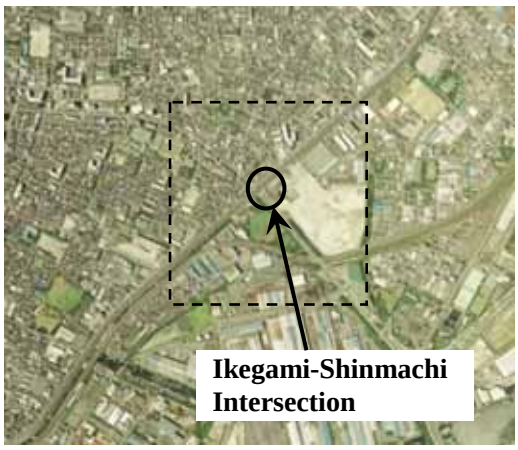

Fig. 1 Objective domain in Kawasaki city

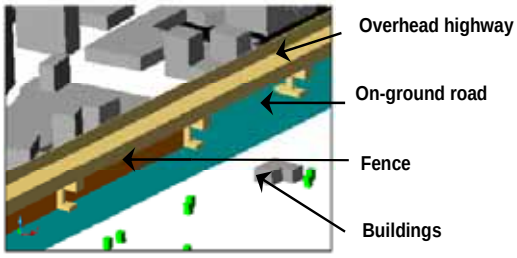

Fig. 2 Geometric Configuration near the Ikegami-Shinmachi Intersection

large scale of width 920m×800m and 70m in height. The Ikegami-Shinmachi intersection is the center of the analysis domain, through out which a SW-NE direction trunk road and an elevated expressway –the Capital Expressway run throughout. The trunk road lies on ground while expressway flies over at height of 8m. There are also several pieces of fence installed under part of the expressway. Fig. 2 shows the geometric configuration for all building elements near the intersection. The objective is densely populated residential area, most of which is covered by two-storey houses of about 4~5m height. It can be concerned that the topography in the domain is considerably sophisticated.

3.2 Mesh Discretization

In such a complex urban area, the use of an unstructured grid is effective means of conducting a CFD simulation (Huang et al. 2005). The official geographical data of analysis objective provided by Ministry of Land, Infrastructure and Transport of Japan, was employed to set up the geometric frame for mesh discretization. Narrow gaps between real buildings have been modified manually to save on excessive meshes, which only incur additional computational expense.

In this calculation, an unstructured grid system including 2,969,130 meshes was created. The smallest width is about 1.0m near the expressway and intersection.

3.3 Meteorological Condition and Pollutant Intensity

A field survey was carried out on 1st, February ~ 3rd, February, 2005. The measurements were taken at 17 points at 20-minute intervals from 8:45 to 15:05. Pollutant emission rate from vehicular transportation was estimated by investigating the traffic load via a video recording taken from a pedestrian bridge. The main pollutants considered in this study are carbon monoxide (CO) and nitrogen monoxide (NO). The meteorological data used was provided by Kawasaki city observation station.

Since the objective domain is mainly for residential use, only the trunk road and overhead expressway in the SW-NE direction were taken as the sources for pollutants with constant emission intensity during the calculation. Furthermore, it was also assumed that hardly any of the pollutants emitted from the vehicles on the elevated expressway would reach pedestrian level, and thus only the ground level trunk road was considered as an exhaust source (Takahashi et al. 2005).

During simulation in this study, four cases were conducted under the conditions associated with that of

Table 2 Pollutant emission intensity

Case Definition		Predicted emission rate			
		CO[g/m*h]		NO[g/m*h]	
		UP*1	DOWN*2	UP	DOWN
case1	10:45-11:05	2.79	2.26	1.41	1.16
case2	12:45-13:05	2.95	1.81	1.20	0.96
case3	12:45-13:05	3.12	2.04	1.39	0.97
case4	14:45-15:05	3.09	2.10	1.40	0.89

*1 Towards Tokyo City (Northeast)

*2 Towards Yokohama City (Southwest)

Table 3 Meteorological conditions

Case Definition		Meteorological Condition	
		Velocity[m/s]	Wind Direction
case1	10:45-11:05	3.7	W
case2	12:45-13:05	2.7	NW
case3	13:45-14:05	1.9	WNW
case4	14:45-15:05	0.9	SSE

Table 4 Simulation cases for the effect of the atmospheric stability

Case	Atmospheric condition	Inflow air temperature	Ground and wall temperature
case1-1	Stable	10˚C	5˚C
case1-2	Unstable	30˚C	40˚C

Table 5 Analysis condition

Turbulent model	Standard k-ε model
Difference scheme	Second order upwind
Inlet	$U = U_0 \cdot (Z / Z_0)^{1/4}, Z_0 = 16m$ $k = 1.5 \cdot (I \times U)^2, I = 0.1$ $\varepsilon = C_\mu \cdot k^{3/2} / l$ $l = 4(C_\mu \cdot k)^{1/2} Z_0^{1/4} Z^{3/4} / U_0$ (Murakami et al 1988)
Side, sky	Free slip
Wall	Generalized logarithmic law

field survey (2nd, Feb, 2005). The meteorological conditions and pollutants emission intensity are listed out in Table 2 and Table 3, respectively. Here, the thermal effect is not considered, so the atmospheric stability is neutral condition. In order to evaluate the effect of atmospheric stability, the selected stable and unstable conditions shown in Table 4 are simulated. The other conditions are the same as case1 in Table 2

Table 5 shows the analysis conditions. In the equation for calculating the inlet wind velocity profile, U_0 and Z_0 are velocity and height at the representative point. Meteorological data offered by the observation station was surveyed at about 16m height above from ground, thus Z_0=16m. The 'constant flux layer' assumption was adopted to generate turbulent energy k and dissipation rate ε of the inlet boundary. The turbulent intensity 'I' was set to be 10% of the representative velocity –U_0.

CFD simulation was performed using a commercial code - STAR CD. The principle of discretization is obtained by using first-order upwind scheme for the convection term. The pressure and velocity coupling is achieved by the SIMPLE algorithm.

4. RESULT DISCUSSION

4.1 Average Wind Distribution

Fig. 3 presents the CFD simulation results of the wind velocity distribution at a horizontal section of 1.5m height around Ikegagmi-Shinmachi intersection for case1 and case2. In the case of western wind (Fig. 3(a), case1), the average wind velocity in bulk area is about 2.0m/s, while in building colony, it decreases significantly even to a lower magnitude, because of the blocking effect produced by buildings to wind flow. The similar situation appears in case2. In case2 (Fig. 3(b)), where the wind blows in a NW direction, it is parallel with the street canyon. Wind maintains a high velocity as it is flowing until meeting obstacles near the intersection. In the area around orphan buildings, circulation flow occurs in leeward region. Both in case1 and case2, the fences orient against the wind direction, and thus probably produce a greater sheltered area. A low velocity can be observed in the region behind these fences. Since the fences locate right on line source of pollutants, it is likely that such pollutants stagnate and conduce high concentration

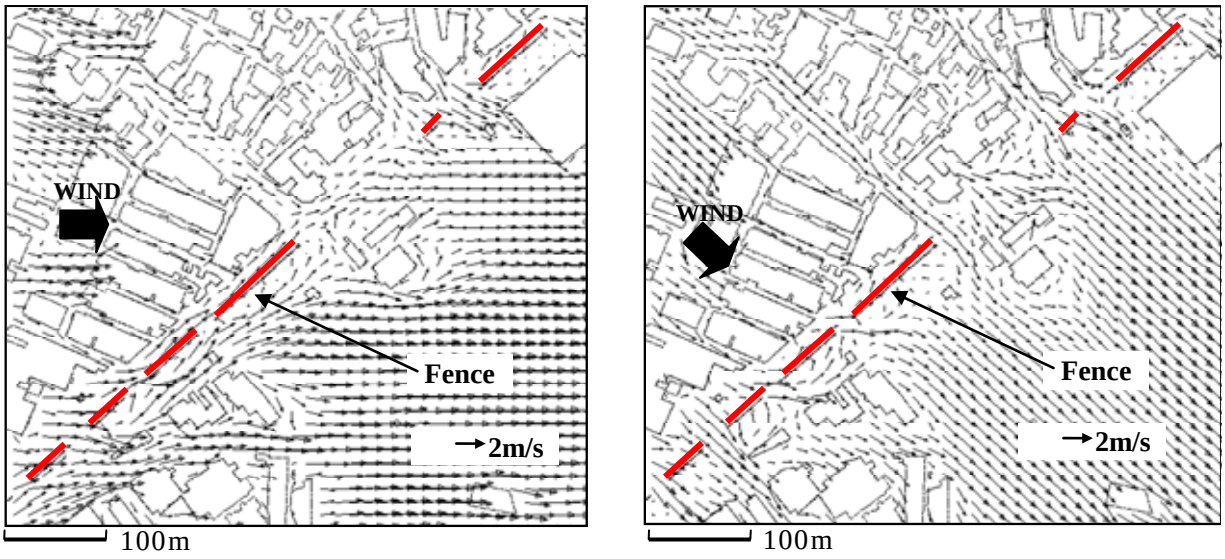

(a) (b)

Fig. 3 Velocity vector distribution: a - case1; b – case2

here.

4.2 Pollutants Dispersion Characteristics

Fig. 4 and Fig. 5 present the pollutants dispersion characteristic under meteorological condition of case1 and case2. Pollutants are first emitted from the traffic road, then transport away with wind flow and disperse in the air. In both case1 and case2, the concentration of both NO and CO are nearly zero in the upstream regions. Contrarily, great range of the downstream area is covered with NO and CO. It should be noted that the concentrations in some upstream areas near the fences appear non-zero concentration because the circulation flow takes place here and transports the pollutants in windward direction. It is illustrated clearly that the concentration of NO and CO in the areas near the emission source-traffic road, are significantly higher than that of any other areas. Concentration decreases gradually as the distance away from trunk road increases in leeward region. In case1, concentration of NO and CO in the downstream place 100m away from the source is 0.03ppm and 0.06ppm, while in case2 0ppm and 0.06ppm. Moreover, the concentrations in the regions behind fences are averagely high due to the low wind velocity and poor ventilation status. Comparatively, in the gaps between two fences where wind can flows through, concentrations are averagely lower. In each case, the emission intensity of CO is about twice that of NO. Accordingly, the average concentration of CO is reasonably greater than NO concentration.

From the discussion above, it is clear that the phenomenon of serious pollution in urban areas depends not only on the escalating emission intensity induced by traffic load, but also result from the unfavorable wind environmental conditions. The fences installed under the expressway obstacle wind flow and cause contaminants to accumulate nearby, which results in excessive pollution problems.

4.3 Validation and the Effect of Atmospheric Stability

Comparing the numerical simulation with the survey data is performed here. The field survey was carried out by measuring the concentrations of NO and CO at the specified points (Nos. 3~ 17), as shown in Fig. 6. During the survey process, not only were the southwest-northeast oriented roads the emission sources, but pollutant exhaust also includes numerous other components, such as roads in other directions. Therefore, it is appropriate to consider the measurement results of the concentration in the upstream area as the background concentration. Here, the background values in case1 are 0.006ppm and 1.15ppm for NO and CO respectively.

The concentrations of NO at each point in case1 (Neutral condition), case1-1 (Stable condition) and case1-2 (Unstable condition) in the CFD simulation and field survey are presented in Fig. 7. It can be seen that there is little difference between neutral condition and stable condition. Therefore, the stable condition is a weak stable condition. Agreement between the case1, case1-1 and field survey results can be seen. Though some disagreement in concentration can be observed at Points 6, 7 and 15, it is considered acceptable from several points.

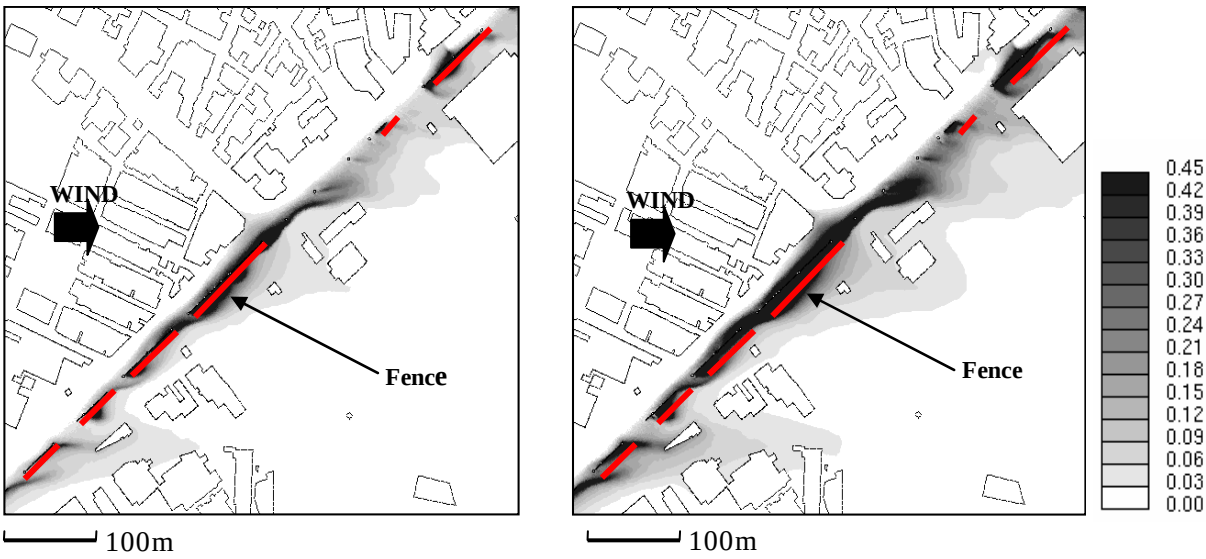

(a) (b)

Fig. 4 Pollutants concentration in case1 (ppm): a – NO; b – CO

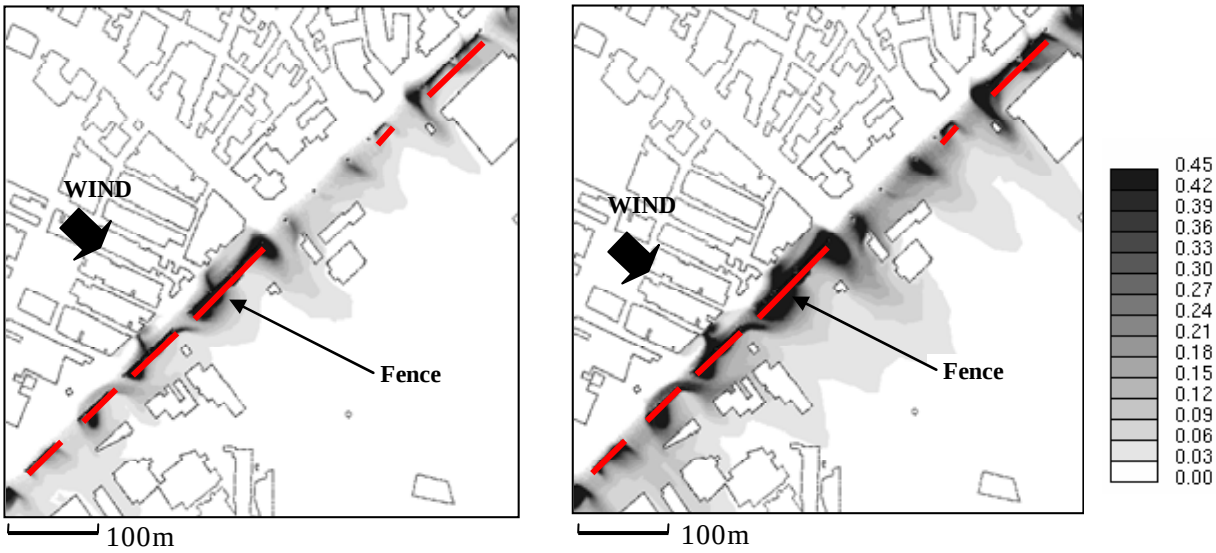

(a) (b)

Fig. 5 Pollutants concentration in case2 (ppm): a – NO; b – CO

The disagreement can be explained as following: there is another trunk road running in SE-NW direction lies within the objective domain, which was not set as a pollutant source in the calculation. Since points 7, 8 and 15 are all very close to that road, it is entirely reasonable to observe a higher concentration in the survey data than the simulation result.

The effect of atmospheric stability on pollutant dispersion can be also known from the Fig. 7. The concentration is the lowest under unstable condition, while it is the highest under stable condition. This is because that the convective mixing is increased under the unstable atmosphere.

5. CONCLUSIONS

In this research, CFD simulation has been carried out to study the air pollutants in a built-up area in Kawasaki city, Japan. The meteorological conditions and pollutant emission intensity associated with that of a field survey was utilized.

The simulation results show the velocity distribution and pollutants dispersion characteristic at pedestrian level. The wind velocity in the buildings colony with high density is averagely very low, which is detrimental to pollutants dispersion. Furthermore, it is known that the regions behind fences are subject to much higher levels of pollutants because of the low local velocity and circulation flow which prevents pollutants from

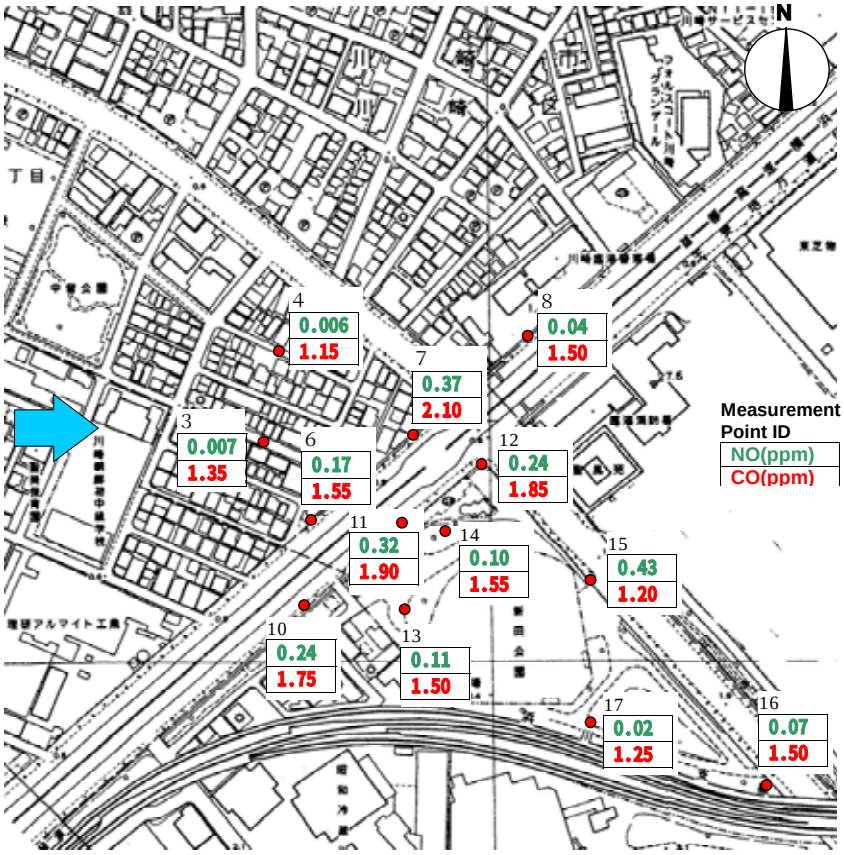

Fig. 6 CO/NO concentration at each point by field survey (case1)

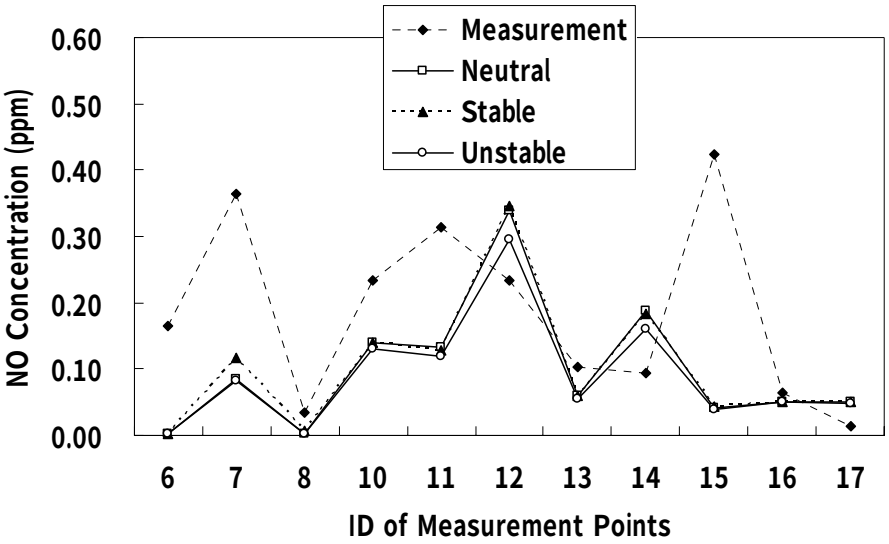

Fig. 7 Comparative study of simulation result and measurement data (NO)

escaping.

The accuracy of the CFD simulation is studied by comparing its results with field survey data. The results show good agreement, thus proving that the CFD method is highly competent in handling complex urban air pollution issues. The effect of atmospheric stability was analyzed. The concentration is the lowest under unstable condition due to the convective mixing, while there is little difference between the neutral condition and stable condition.

References

Huang, H., Akutsu, Y., Arai, M. and Tamura, M., 2000: A two-dimensional air quality model in an urban street canyon: evaluation and sensitivity analysis. *Atmos. Environ.,* 34, 689-698.

Huang, H., Ooka, R. and Kato, S., 2005: Urban thermal environment measurements and numerical simulation for an actual complex urban area covering a large district heating and cooling system in summer, *Atmos. Environ.*, 39, 6362-6375, 2005.

Kim, J. and Baik, J., 2001: Urban street-canyon flows with bottom heating. *Atmos. Environ*., 35, 3395-3404.

Kim, S.E., 1999: Application of CFD to environmental flows. *J. Wind and Ind. Aerodyn.*, 81, 145-158.

Gosman, A. D., 1999: Developments in CFD for industrial and environmental applications in wind engineering. *J. Wind and Ind. Aerodyn.*, 81, 21-39.

Launder, B.E. and Spalding, D.B., 1974: The numerical computation of turbulent flows. *Computer methods in applied mechanics and engineering*, 3, 269-289.

Nakamura, Y. and Oke, T. R., 1988: Wind, temperature and stability conditions in an east-west oriented urban canyon. *Atmos. Environ.*, 22, (12), 2691-2700.

Takahashi, T., Kato S., Ooka, R., Kono, R. and Watanabe, T., 2005: Prediction of Pollutant Dispersion Caused by Automotive Exhaust- A Comparison between Field Measurements and Wind Tunnel Data. *The Sixth Asia-Pacific Conference on Wind Engineering, Submitted, Seoul, Korea,* Sep. 12-14, Korea.

Murakami, S., 1990: Numerical simulation of turbulent flow field around cubic model current status and applications of k-ε model and LES, *J. Wind and Ind. Aerodyn.*, 33, 139-152.

Murakami, S., Mochida, A. and Hayashi, Y., 1988: Modification of production terms in k-ε Model to remove overestimate of k value around windward corner. *10th Wind Engineering Symposium*, 199-204. (In Japanese)

Vardoulakis, S., Fisher, B. E. A., Pericleous, K., and Gonzalez-Flesca, N., 2003: Modeling air quality in street canyons: a review. *Atmos. Environ.*, 37, 155-182.